Journal of Physiology and Biochemistry (2023) 79:341–353
https://doi.org/10.1007/s13105-023-00945-5

ORIGINAL ARTICLE

Klotho improves cardiac fibrosis, inflammatory cytokines, ferroptosis, and oxidative stress in mice with myocardial infarction

Kai WANG[1] · Zhongming LI[2] · Yinzhang DING[1] · Zheng LIU[1] · Yansong LI[2] · Xianling LIU[2] · Yan SUN[2] · Jian HONG[2] · Wei ZHENG[1] · Lijun QIAN[2] · Di XU[2]

Received: 8 September 2022 / Accepted: 16 January 2023 / Published online: 26 January 2023

Abstract

The anti-aging protein Klotho has been associated with cardiovascular health protection. Nevertheless, the protective mechanism remains unknown. The present study is aimed at exploring the effect of Klotho on cardiac remodeling and its potential mechanism in mice with myocardial infarction (MI). We used left anterior coronary artery descending ligation to develop an MI model for in vivo analyses. In contrast, H9C2 cells and cardiac fibroblasts were used to establish the oxygen–glucose deprivation (OGD) model in in vitro analyses. In vivo and in vitro models were treated with Klotho. Compound C, an AMPK signaling inhibitor, was used to determine whether Klotho's effects are mediated through the AMPK/mTOR signaling pathway. Echocardiography, Masson trichrome staining, immunofluorescence, immunohistochemistry, real-time polymerase chain reaction (RT-PCR), and western blot were used to detect the related indicators. The findings of the in vivo model indicate that Klotho treatment improved the mice's cardiac function, reduced cardiac fibrosis, and attenuated myocardial inflammatory factors, ferroptosis, and oxidative stress. The results of the in vitro model were in line with the findings of in vivo modeling. An AMPK inhibitor, Compound C, reversed all these effects. In conclusion, Klotho potentially improves cardiac remodeling in MI mice by regulating AMPK/mTOR signaling, demonstrating Klotho as an effective MI therapeutic agent.

Keywords Klotho · Myocardial infarction · Cardiac fibrosis · Inflammatory cytokines · Ferroptosis · Oxidative stress · AMPK/mTOR signaling pathway

Kai WANG, Zhongming LI, and Yinzhang DING contributed equally to this work.

Keypoints.

Klotho ameliorates cardiac function, reduces cardiac fibrosis, and attenuates myocardial inflammatory factors in mice with myocardial infarction.

Klotho improves ferroptosis and oxidative stress in mice with myocardial infarction.

Klotho potentially improves cardiac remodeling in MI mice by regulating AMPK/mTOR signaling.

✉ Di XU
xudi@jsph.org.cn

[1] Department of Cardiology, The First Affiliated Hospital of Nanjing Medical University, No. 300 Guangzhou Road, Nanjing 210029, Jiangsu, China

[2] Department of Geriatrics, The First Affiliated Hospital of Nanjing Medical University, No. 300 Guangzhou Road, Nanjing 210029, Jiangsu, China

Introduction

Myocardial infarction (MI) is a severe cardiac disorder associated with high rates of hospitalization and death [1]. Even with medication and coronary intervention, the prognosis for patients with MI remains poor at the moment [2]. Cardiac remodeling, including cardiac fibrosis [3], inflammatory cytokine–induced inflammation [4], ferroptosis [5], and oxidative stress [6], plays a significant role in the development of heart failure following MI.

Klotho, an anti-aging protein discovered in 1997, has been linked to the aging process in humans [7]. Klotho has been shown to protect against vascular calcification in chronic kidney disease [8]. Besides, Klotho is associated with diabetes mellitus [9]. Recently, multiple pieces of evidence revealed that Klotho has cardioprotective effects. Chen et al. found that its deficiency impairs Nrf2-GR pathway activity, resulting in heart aging [10]. Furthermore, it could protect the heart from hyperglycemia-induced injury by inhibiting reactive oxygen species (ROS) and

NF-κB-mediated inflammation [11]. Our previous study also confirmed the cardioprotection of Klotho by inducing autophagy [12]. However, the effects of Klotho on mice with MI are rarely investigated.

The AMPK/mTOR signaling pathway is closely related to cardiac remodeling after MI [13]. Lu et al. revealed that activating AMPK signaling can modulate myocardial contractility and reduce myocardial infarct size [14]. Besides, promoting AMPK phosphorylation may reduce cardiac apoptosis and infarction area and improve mice's heart function in acute MI [15]. In addition, by targeting the AMPK-mTOR signaling pathway, cardiac dysfunction following myocardial infarction could be improved [16]. However, it is unknown whether Klotho can improve cardiac remodeling after MI by regulating AMPK/mTOR signaling. The present study investigates the role of Klotho on cardiac remodeling and possible mechanisms in mice with MI.

Material and methods

Animals and experimental design

A total of 27 male C57BL/6 mice (6 weeks) were obtained from Weitong Lihua Limited Company (Beijing, China) and acclimatized for 1 week. A 12-h light–dark cycle was maintained at 22–24 °C, and all animals had unrestricted access to food and water. After 1 week of adaptation, the MI surgery was performed on 22 mice, while the sham surgery was performed on five mice. The surgical procedure was performed as previously described [1]. Briefly, mice were anesthetized with pentobarbital sodium (45 mg/kg). The heart was then exposed by opening the chest at the second and third intercostal muscles. Arterial ligation of the left anterior descending coronary (LAD) artery was performed with silk sutures of 7–0 gauge. In sham mice, simulated surgical procedures were performed on mice without LAD ligation. After a week, all mice with a sham MI operation survived, whereas 17 mice with an MI operation survived. Then, we performed echocardiography to confirm the success of the model. The mice were randomly divided into the sham group ($n=5$), the MI group ($n=6$), the MI + K group ($n=5$), and the MI + K + CC group ($n=6$). Sham mice and MI mice were given 5 mL/kg saline intraperitoneally every other day for 28 days. According to a previous study [17], mice in the MI + K group were given 20 μg/kg Klotho protein (R&D, cat. number: 1819-KL-050) intraperitoneally every other day for 28 days. An aqueous solution of Klotho protein (4 μg/mL) was dissolved in sterile water. Compound C, an AMPK signaling inhibitor, was used to determine whether Klotho's effects are mediated by AMPK/mTOR signaling. MI + K + CC group mice were given 20 μg/kg Klotho protein and 5 mg/kg Compound C (APExBIO, cat. number: B3252) intraperitoneally every other day for 28 days. The dose of Compound C was selected based on a previous study [18].

Echocardiography

The cardiac function indicators, including left ventricular ejection fraction (LVEF) and left ventricular fractional shortening (LVFS), were obtained 1 week and 5 weeks after MI. All mice were anesthetized with isoflurane, and echocardiographic measurements were conducted using the Vevo3100 Echocardiography System (VisualSonics, Toronto, Canada). Echocardiography parameters were obtained based on a previous study [19].

Histology and immunohistochemistry

At the end of the study, all mice were euthanized with an overdose of pentobarbital sodium (200 mg/kg). We collected left ventricular (LV) tissues and blood samples. A portion of LV tissues was fixed in formalin and processed for histology and immunohistochemistry. Another portion of LV was used for western blot and real-time PCR. We cut formalin-fixed paraffin-embedded mid-transverse LV sections in 5-μm-thick slices. Then, the 5-μm-thick specimens were stained with Masson trichrome staining and examined under the light microscope for myocardial fibrosis. A blinded method of observation and counting myocardial fibrosis was employed by two observers independently in five randomly selected fields. The ratio of collagen surface area to the total surface area was used to calculate the extent of cardiac fibrosis in the left ventricular peri-infarct region [1]. Collagen I (Coll-1) antibodies (Proteintech, China, 1:500) were used in the immunostaining of paraffin-embedded heart sections, as previously reported [20]. The sections were then incubated with secondary antibodies. After incubation with a peroxidase substrate (DAB) kit, the visual fields of each section were photographed and analyzed with the ImageJ software. Collagen I expression area ratios were calculated by dividing the collagen I area by the total visual field area [21].

Cell culture

The rat cardiomyocyte H9C2 cells, provided by Cell Bank (Shanghai, China), were cultured in 10% FBS-containing DMEM. As described previously, MI was mimicked in vitro using an oxygen–glucose deprivation (OGD) model [22]. We divided H9C2 cells into the sham, the OGD, the OGD + K, and the OGD + K + CC group. The Klotho protein was dissolved in sterile water at a concentration of 0.4 nmol/L [12, 17]. Klotho was administered at 0.4 nmol/L 30 min before OGD induction in the OGD + K group. Klotho and Compound C were administered to the OGD + K + CC

group 30 min before OGD induction, at a concentration of 0.4 nmol/L and 10 μM, respectively [23].

Cardiac fibroblast isolation and culture

Cardiac fibroblasts (CFs) were isolated from the hearts of C57BL/6 mice (aged 1–3 days) using a previously described differential adhesion technique [24]. Briefly, hearts were extracted from neonatal mice and cut into small pieces under aseptic conditions. The cardiac tissue was then digested with a 0.25% trypsin solution at 37 °C, followed by dissociation with collagenase type 2. Cell suspensions were filtered through 200-mm cell strainers before centrifugation at 1000 rpm for 5 min.

The cells were then resuspended in DMEM supplemented with 10% FBS and 1% penicillin/streptomycin. Due to the different wall adherence durations of CFs and cardiomyocytes, 1.5 h of differential adhesion was performed to obtain CFs. Following a 12-h incubation with a serum-free medium, CFs were treated with glucose-free DMEM and incubated for 12 h in a mixed gas chamber (0.1% O_2, 94.9% N_2, and 5% CO_2) at 37 °C to construct the OGD model [22, 25]. CFs were treated with Klotho (0.4 nmol/L) and Compound C (10 μM) 30 min before OGD induction.

SOD and MDA activity

Serum was separated from blood samples by centrifugation at 3000 rpm at 4 °C for 10 min and then stored at − 80 °C for the remaining biochemical analysis. As indicators of oxidative stress, superoxidase dismutase (SOD) levels and malondialdehyde (MDA) levels were measured. To measure SOD levels and MDA levels, an appropriate biomedical detection (Nanjing Jiancheng Biological Product, Nanjing, China) was prepared. In brief, the serum was first mixed with the reaction solution and then incubated at 37 °C for 40 min. The activities of SOD and MDA were measured using spectrophotometric methods.

Measurement of ROS

Reactive oxygen species (ROS) were measured in H9C2 cardiomyocytes. We detected ROS generation in situ using dihydroethidium (DHE, Beyotime Institute of Biotechnology, China), a fluorescent superoxide-anion probe. The DHE assay was performed following the manufacturer's instructions. Briefly, DHE was diluted with DMSO to a final concentration of 5 μM. After the treatment, the fluorescence assay followed 30-min incubation with DHE at 37 °C. ROS were detected by excitation at 488 nm and emission at 525 nm using fluorescence signals. The cells were then analyzed by using a fluorescence microscope. We randomly selected 5 fields from each group and used the ImageJ software to quantify the fluorescence density.

Immunofluorescence analysis

CFs were seeded in 24-well chambers and allowed to form a monolayer. The cells were then fixed in 4% paraformaldehyde for 30 min and permeabilized with 0.1% Triton X-100 for 15 min. We blocked the cells with 10% donkey serum at room temperature for 30 min and then incubated overnight at 4 °C with primary antibodies against a-SMA (Proteintech, China, 1:200). After incubation with the appropriate secondary antibody conjugated with HRP, the cells were incubated for 1 h at 37 °C the following day. The nuclei were stained with DAPI. Six to ten fields of view were selected randomly under fluorescence microscopy, and representative images were captured.

Real-time PCR (RT-PCR)

Total RNA was isolated from peri-infarct myocardial tissues and H9C2 cells with TRIzol (Invitrogen) as directed by the manufacturer. We defined cyanotic tissue and scar tissue as areas of myocardial infarction. The tissues surrounding the cyanotic tissue and scar tissue were the peri-infarct myocardial tissues. The HiScript II R Transcriptase Kit (Vazyme Biotech Co., Ltd. China) was used to R transcribe the total RNA into cDNA. Subsequently, the ChamQ SYBR qPCR master mix (Vazyme Biotech Co., Ltd., China) was used for RT-qPCR. The Ct value of each target gene was normalized to the Ct value of GAPDH/β-ACTIN (ΔCt). Relative gene expression values were calculated as $2^{-\Delta Ct}$ [26]. The reference gene was GAPDH or β-ACTIN. The primer sequences for mouse were as follows: atrial natriuretic peptide (ANP), forward (F) 5′-GCTTCCAGGCCATATTGGAG-3′ and reverse (R) 5′-GGGGGCATGACCTCATCTT-3′; brain natriuretic peptide (BNP), F 5′-GAGGTCACTCCTATCCTCTGG-3′ and R 5′-GCCATTTCCTCCGACTTTTCTC-3′; collagen I, F 5′-GCTCCTCTTAGGGGCCACT-3′ and R 5′-CCACGTCTCACCATTGGGG-3′; collagen III (Coll-3), F 5′-CTGTAACATGGAAACTGGGGAAA-3′ and R 5′-CCATAGCTGAACTGAAAACCACC-3′; GAPDH, F 5′-AGGTCGGTGTGAACGGATTTG-3′ and R 5′-GGGGTCGTTGATGGCAACA-3′; IL-1β, F 5′-GCAACTGTTCCTGAACTCAACT-3′ and R 5′-ATCTTTTGGGGTCCGTCAACT-3′; IL-6, F 5'-TAGTCCTTCCTACCCCAATTTCC-3′ and R 5′-TTGGTCCTTAGCCACTCCTTC-3′; TGF-β1, F 5′-CCACCTGCAAGACCATCGAC-3′ and R 5′-CTGGCGAGCCTTAGTTTGGAC-3′; TNF-α, F 5′-CAGGCGGTGCCTATGTCTC-3′ and R 5′-CGATCACCCCGAAGTTCAGTAG-3′; ICAM-1, F 5′-GGCATTGTTCTCTAATGTCTCCG-3′ and R 5′-TGTCGAGCTTTGGGATGGTAG-3′; VCAM-1, F 5′-AGTTGGGGATTCGGTTGTTCT-3′ and

R 5′-CCCCTCATTCCTTACCACCC-3′; GPX4, F 5′-TTCTCAGCCAAGGACATCG-3′ and R 5′-CACTCAGCATATCGGGCAT-3′; ASCL4, F 5′-GTGCCGCGAAGTTAATG-3′ and R 5′-CAAAGGTTAGACGGGATGA-3′; and SOD-1, F 5′-GGTTCCACGTCCATCAGT-3′ and R 5′-ACATTGCCCAGGTCTCC-3′. The primer sequences for rats were as follows: IL-1β, F 5′-CCACATCCCTGTTACCTGA-3′ and R 5′-TGACACCCTGGTTTGAGAA-3′; IL-6, F 5′-AGGAGTGGCTAAGGACCAAGACC-3′ and R 5′-TGCCGAGTAGACCTCATAGTGACC-3′; β-ACTIN, F 5′-TGCTATGTTGCCCTAGACTTCG-3′ and R 5′-GTTGGCATAGAGGTCTTTACGG-3′; TGF-β1, F 5′-CCTACATTTGGAGCCTGGA-3′ and R 5′-CCGGGTTGTGTTGGTTG-3′; TNF-α, F 5′-CAGCCAGGAGGGAGAAC-3′ and R 5′-GTATGAGAGGGACGGAACC-3′; ICAM-1, F 5′-CCAGCCCCTAATCTGACCT-3′ and R 5′-CTAAAGGCACGGCACTTGT-3′; and VCAM-1, F 5′-GAAATGCCACCCTCACC-3′ and R 5′-GAATCCCCAACCTGTGC-3′.

Western blot

Proteins were extracted from peri-infarct myocardial tissue and H9C2 cells. We used a BCA kit (Beyotime Institute of Biotechnology, China) to determine the protein concentration. Protein samples were separated by gel electrophoresis in 10% SDS–polyacrylamide gel and transferred to polyvinylidene fluoride membranes. After blocking with 5% skim milk, the membranes were incubated overnight with primary antibodies, including GPX4 (Proteintech, China, 1:2000), AMPK (Proteintech, China, 1:2000), P-AMPK (Immunoway, China, 1:1000), mTOR (Proteintech, China, 1:5000), P-mTOR (Cell Signaling Technology, USA, 1:1000), ASCL4 (ABclonal, China, 1:2000), and GAPDH (Proteintech, China, 1:5000). After that, the membranes were incubated at room temperature for 2 h with the secondary antibody. The blots were analyzed with the ImageJ software.

Statistical analysis

The data were presented as mean ± standard error. GraphPad Prism software (GraphPad Software, USA) was used to analyze the data. One-way analysis of variance (ANOVA) was used for statistical analysis, followed by Tukey's multiple comparison test. Statistics were considered significant when the P value was < 0.05.

Results

MI caused adverse cardiac function

Echocardiography was performed 1 week after MI to determine whether the mouse model in this study had been successfully established. MI mice, MI + K mice, and MI + K + CC mice had significantly lower EF and FS than sham mice. Furthermore, there were no differences in EF and FS between the MI, MI + K, and MI + K + CC groups. Figure 1A–C represents cardiac function from mice assigned to these groups prior to being treated with the Klotho and Compound C. All of these indicated the establishment of a successful MI model.

Effects of Klotho on cardiac function in mice with MI

Five weeks after MI, five mice survived in each of the four groups (sham, MI, MI + K, and MI + K + CC). The MI group significantly had decreased EF and FS compared to the sham group. Nonetheless, mice in the MI + K group had higher EF and FS than mice in MI and MI + K + CC groups (Fig. 1D–F). Furthermore, when the MI and MI + K + CC groups were compared, the expression of ANP and BNP mRNA in MI + K mice was lower (Fig. 1G, H).

Effects of Klotho on myocardial fibrosis in mice with MI

Masson trichrome staining and Coll-1 immunohistochemistry were used to assess the degree of myocardial fibrosis 5 weeks after MI. In contrast to sham mice, MI mice and MI + K + CC mice had significant myocardial fibrosis as determined by Masson staining, while the degree of cardiac fibrosis was significantly reduced by Klotho treatment. The Coll-1 immunohistochemistry results were consistent with the Masson staining results. In addition, MI + K mice had lower levels of Coll-1 and Coll-3 mRNA than MI and MI + K + CC mice (Fig. 2).

Effects of Klotho on inflammatory factors and oxidative stress in mice with MI and effects of Klotho on the ROS of H9C2 cells

In the present study, we measured the levels of TGF-β1, TNF-α, VCAM-1, MCP-1, ICAM-1, IL-1β, and IL-6 mRNA. The MI and MI + K + CC groups had higher levels of inflammatory factors (IL-1β, IL-6, TGF-β1, TNF-α, VCAM-1, and ICAM-1) than the MI + K and sham groups (Fig. 3A, B). To explore the level of oxidative stress, we measured SOD, MDA, and ROS expression. Compared to the MI and MI + K + CC groups, the MI + K group had significantly higher SOD and SOD-1 mRNA levels. However, compared to the MI + K and sham groups, there was a significant increase in the MDA levels in the MI and MI + K + CC groups (Fig. 3E–G). In addition, compared to the OGD and OGD + K + CC groups, Klotho treatment reduced the ROS fluorescence intensity (Fig. 3C, D).

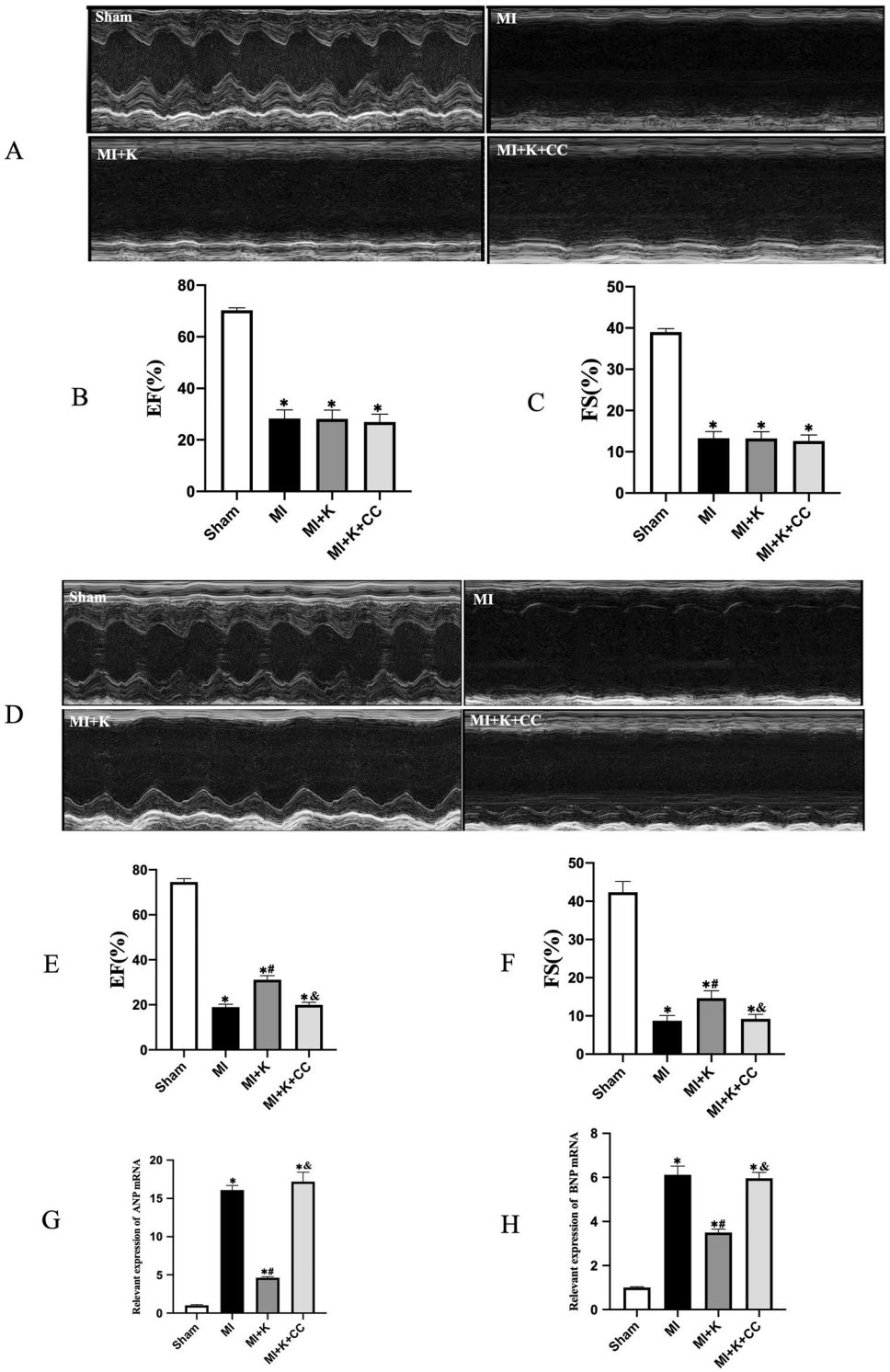

Fig. 1 Results of echocardiography in mice 1 week and 5 weeks after MI. **A** Representative echocardiographic image of the left ventricular at 1 week post-MI. **B** Left ventricular ejection fraction 1 week after MI. **C** Left ventricular fractional shorting 1 week after MI. One week after MI, there were 5, 6, 5, and 6 mice in sham, MI, MI + K, and MI + K + CC groups, respectively. **D** Representative echocardiographic image of the left ventricular 5 weeks after MI. **E** Left ventricular ejection fraction 5 weeks after MI. **F** Left ventricular fractional shorting 5 weeks after MI. Expressions of ANP (**G**) and BNP (**H**) mRNA. Five weeks after MI, there were 5, 5, 5, and 5 mice in sham, MI, MI + K, and MI + K + CC groups, respectively. Data are mean ± SEM. $^{*}P < 0.05$ vs. sham. $^{\#}P < 0.05$ vs. MI. $^{\&}P < 0.05$ vs. MI + K. MI, myocardial infarction; K, Klotho; CC, Compound C; ANP, atrial natriuretic peptide; BNP, brain natriuretic peptide

Effects of Klotho on ferroptosis and AMPK/mTOR signaling in mice with MI

The expression of ACSL4 and GPX4 presents the levels of ferroptosis. The effect of Klotho on ferroptosis in MI mice was investigated in the present study. According to western blot results, the MI and MI + K + CC groups had higher ASCL4 expression than the MI + K and the sham groups. Furthermore, the GPX4 expression in MI + K mice was higher than that in MI and MI + K + CC mice (Fig. 4A, B).

Similarly, the mRNA level of ASCL4 was consistent with the western blot results. MI + K mice had higher expression

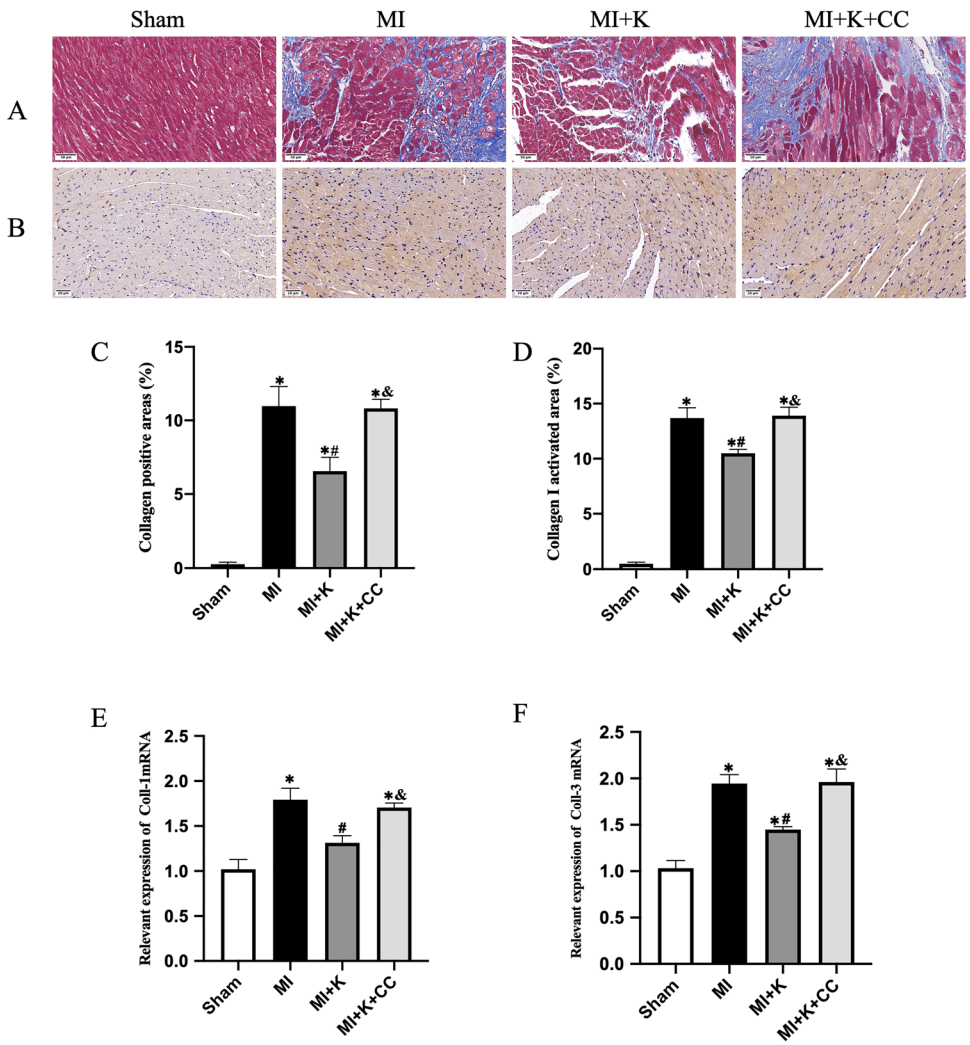

Fig. 2 Effects of Klotho on cardiac fibrosis in mice with MI. **A** Masson trichrome staining of heart tissue. Blue indicates fibrotic regions; scale bar: 50 μm. **B** Immunohistochemistry staining of collagen I in heart tissues; scale bar: 20 μm. **C** The ratio of fibrosis area to total area. **D** The ratio of Coll-1-positive area to total area; expressions of Coll-1 (**E**) and Coll-3 (**F**) mRNA. $N = 5, 5, 5,$ and 5 in sham, MI, MI + K, and MI + K + CC groups, respectively. Data are mean ± SEM. $^{*}P < 0.05$ vs. sham. $^{\#}P < 0.05$ vs. MI. $^{\&}P < 0.05$ vs. MI + K. MI, myocardial infarction; K, Klotho; CC, Compound C; Coll-1, collagen I; Coll-3, collagen

of GPX mRNA than MI and MI + K + CC mice (Fig. 4C). Moreover, the effects of Klotho on AMPK/mTOR signaling were investigated. The MI and MI + K + CC groups had lower levels of phosphorylated AMPK expression than the MI + K and sham groups. The P-AMPK/AMPK ratio was consistent with the P-AMPK expression. In addition, the P-mTOR/mTOR ratio was lower in the MI + K group than the MI and MI + K + CC groups. However, no statistically significant differences in AMPK expression were found among these four groups (Fig. 4D–H).

Effects of Klotho on cardiac fibrosis and inflammatory cytokines in vitro

Furthermore, we explored the effects of Klotho on inflammatory cytokines in H9C2 cells and the level of fibrosis in CFs. The PCR results showed that the OGD + K group had lower levels of inflammatory factors (IL-1β, IL-6, TGF-β1, TNF-α, VCAM-1, and ICAM-1) than the OGD and OGD + K + CC groups (Fig. 5A, B). Compared to OGD and OGD + K + CC groups, the OGD + K group had a lower expression of α-SMA (Fig. 5C–E).

Effects of Klotho on ferroptosis and AMPK/mTOR signaling in vitro

The effects of Klotho on ferroptosis and AMPK/mTOR signaling in H9C2 cells were also investigated. The ASCL4 expression in the OGD + K group was lower than that in the OGD and OGD + K + CC groups. A higher expression of GPX4 was observed in the OGD + K group compared to the OGD and OGD + K + CC groups (Fig. 6A–C). Furthermore, compared with the OGD + K group, there was a decrease in P-AMPK expression, and the ratio of P-AMPK to AMPK was observed in the OGD and OGD + K + CC groups. Additionally, the ratio of P-mTOR to mTOR was lower in the OGD + K group than in the OGD and OGD + K + CC groups. However, there was no difference in the expression of AMPK among these four groups (Fig. 6D–G).

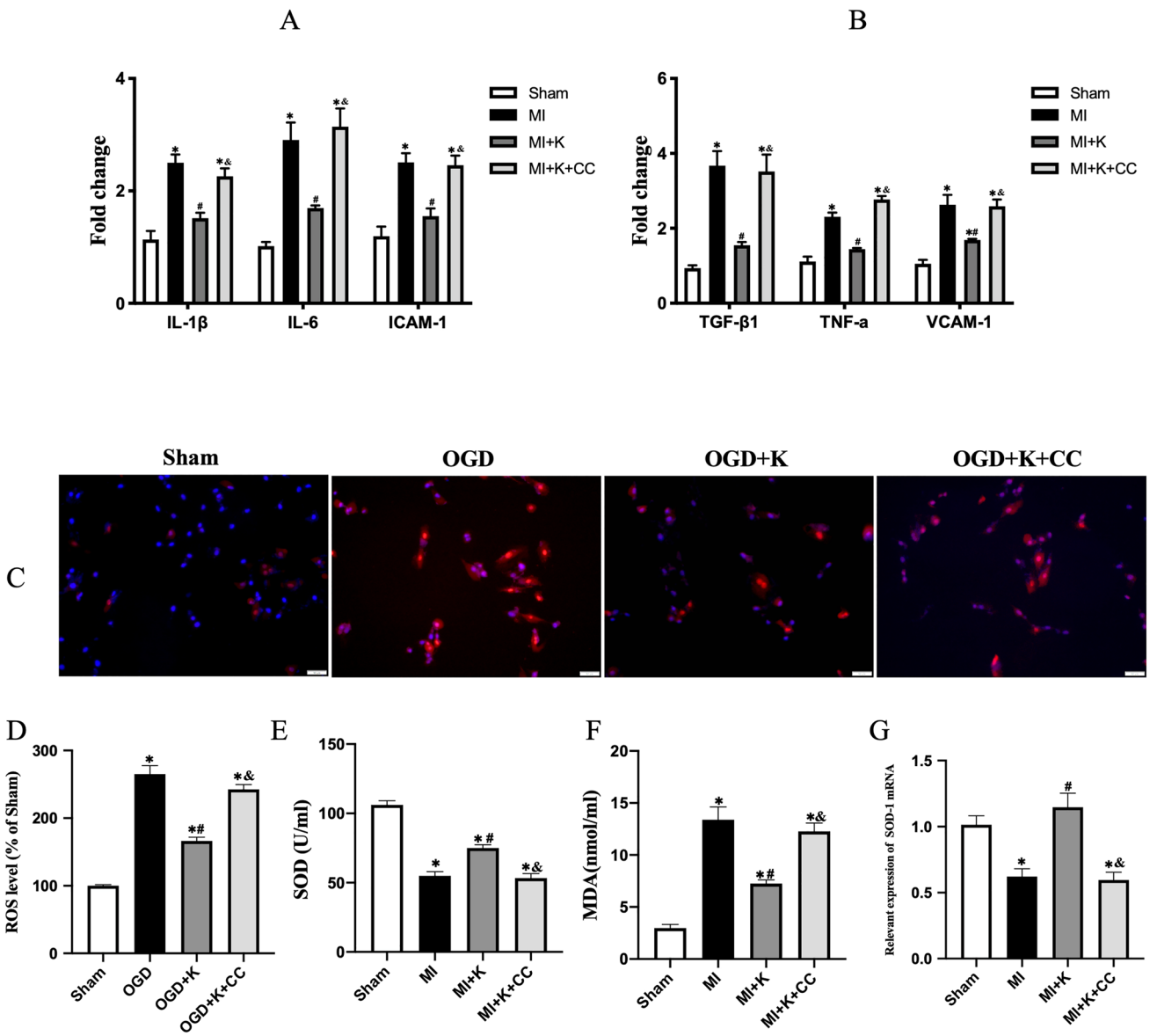

Fig. 3 Effects of Klotho on inflammatory factors and oxidative stress in mice with MI and effects of Klotho on the ROS of H9C2 cells. **A** Expression of IL-1β, IL-6, and ICAM-1 mRNA. **B** Expression of TGF-β1, TNF-α, and VCAM-1 mRNA. **C** Fluorescence images of intracellular ROS of H9C2 cells, staining with DHE. **D** The levels of ROS of H9C2 cells. The levels of SOD (**E**) and MDA (**F**). **G** Expression of SOD-1 mRNA. $N=5$, 5, 5, and 5 in sham, MI, MI + K, and MI + K + CC groups, respectively. Data are mean ± SEM. $^{*}P<0.05$ vs. sham. $^{\#}P<0.05$ vs. MI/OGD. $^{\&}P<0.05$ vs. MI + K/OGD + K. MI, myocardial infarction; OGD, oxygen–glucose deprivation; K, Klotho; CC, Compound C; ROS, reactive oxygen species; DHE, dihydroethidium; SOD, superoxidase dismutase; MDA, malondialdehyde

Discussion

MI is a serious global disease associated with high morbidity and mortality rates [27, 28]. Klotho has a cardioprotective role in MI patients [29]. However, the underlying mechanisms are still unknown. In the present study, we established an MI model. We found that (1) Klotho treatment improves cardiac fibrosis, inflammatory cytokines, ferroptosis, and oxidative stress in vivo and in vitro and (2) the Klotho treatment may exert its beneficial effect through the activity of the AMPK/mTOR signaling pathway.

Myocardial fibrosis plays a significant role in cardiac remodeling, contributing to heart failure and death [30]. Moreover, cardiac fibrosis is associated with an increase in the incidence of malignant arrhythmias, which ultimately increases patient mortality [31, 32]. In this study, we found that Klotho could reduce the severity of myocardial fibrosis both in vivo and in vitro; this indicates that Klotho may reduce the incidence of malignant arrhythmias in MI

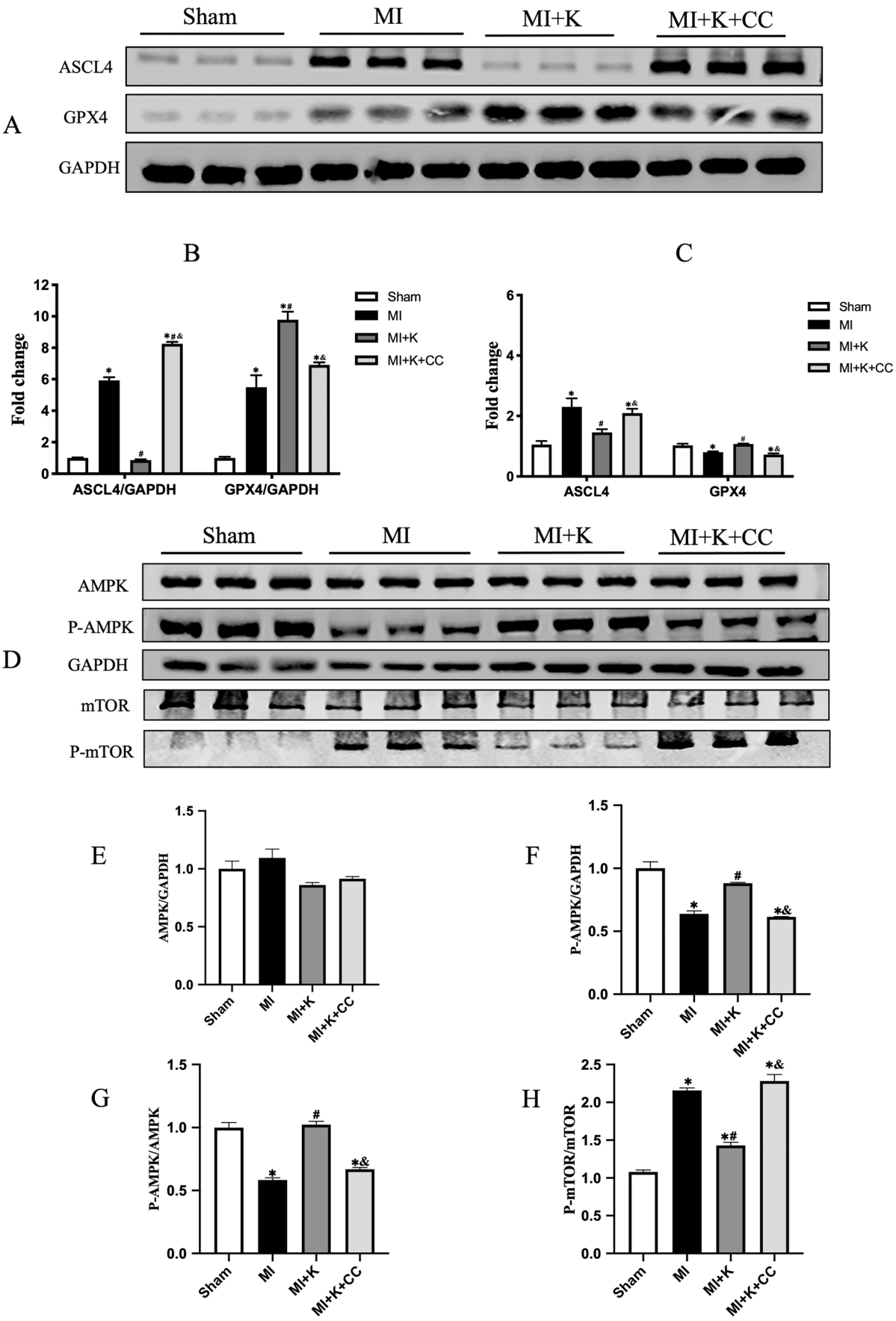
A
Sham
MI
MI+K
MI+K+CC
ASCL4
GPX4
GAPDH
B
Fold change
ASCL4/GAPDH
GPX4/GAPDH
C
Fold change
ASCL4
GPX4
Sham
MI
MI+K
MI+K+CC
D
AMPK
P-AMPK
GAPDH
mTOR
P-mTOR
E
AMPK/GAPDH
F
P-AMPK/GAPDH
G
P-AMPK/AMPK
H
P-mTOR/mTOR

◂**Fig. 4** Effects of Klotho on ferroptosis and AMPK/mTOR signaling in mice with MI. **A**, **B** Western blot analysis of the expressions of ASCL4 and GPX4. **C** Expressions of ASCL4 and GPX4 mRNA. **D–H** Western blot analysis of the expressions of AMPK/mTOR signaling. $N = 5$, 5, 5, and 5 in sham, MI, MI + K, and MI + K + CC groups, respectively. Data are mean ± SEM. $^{*}P < 0.05$ vs. sham. $^{\#}P < 0.05$ vs. MI. $^{\&}P < 0.05$ vs. MI + K. MI, myocardial infarction; K, Klotho; CC, Compound C

patients. Inflammation significantly affects cardiac remodeling and outcome after MI [33]. A previous study showed that the inhibition of IL-1β could protect cardiomyocytes from infarction [34]. A high IL-6 level has been associated with larger infarcts and decreased cardiac function in MI patients [35].

Furthermore, TNF-α may cause myocardial remodeling in heart failure [36]. Inhibiting the TGF-β1/Smads pathway may help to alleviate heart failure caused by MI [37]. In addition, there is a link between lower levels of VCAM-1 and ICAM-1 and better cardiac function [38]. The present study found that Klotho treatment could reduce inflammatory cytokines. Thus, Klotho may have the potential to improve the prognosis of MI patients.

Ferroptosis is a type of regulated cell death characterized by iron overload, resulting in the accumulation of lethal levels of lipid hydroperoxides [5]. It was found in a previous study that ferroptosis was present in cardiomyocytes of MI, and inhibiting ferroptosis improved MI pathology [39]. ASCL4 and GPX4 were markers representing the ferroptosis levels [40]. An enzyme named ASCL4 is involved in phospholipid metabolism. It affects ferroptosis by catalyzing the formation of polyunsaturated fatty-acid-acyl-CoA [41], which are the major substrates of ferroptotic lipid peroxidation [42]. GPX4 exerts a significant role in the regulation of ferroptosis. The inhibition of GPX4 or the synthesis of glutathione (GSH) which is an essential cofactor for GPX4 function could initiate ferroptosis [5]. It was found that Klotho could inhibit the ASCL4 expression while increasing GPX4 expression; this indicates that Klotho could inhibit ferroptosis. It suggests that Klotho could improve cardiac remodeling in MI patients. Our results were consistent with previous studies [43]. ROS, SOD, and MDA presented the levels of oxidative stress. Higher levels of oxidative stress have been associated with adverse cardiac remodeling [44]. A streptozotocin-induced diabetic rat model shows that Klotho suppresses oxidative stress and inflammation in the lens, thereby preventing cataract development and progression [45]. Similarly, in our study, Klotho treatment decreased the levels of ROS and MDA and increased the level of SOD, which suggests the beneficial effects of Klotho on cardiac remodeling in mice with MI.

The AMPK/mTOR signaling pathway, which regulates cell growth, autophagy, and metabolism [46–48], is important in MI development [13, 49]. There are lots of studies showing that the AMPK/mTOR signaling pathway is associated with cardiac function, fibrosis, inflammatory factors, ferroptosis, and oxidative stress. Yan et al. revealed that spermidine improved MI-induced cardiac dysfunction, cardiac fibrosis, cardiac oxidative stress, and inflammatory reaction by promoting AMPK/mTOR mediated autophagic flux [16]. Besides, dexmedetomidine could attenuate ferroptosis induced by myocardial ischemia/reperfusion via AMPK signaling [50]. In addition, Klotho could protect against diabetic kidney disease via AMPK signaling [51]. However, there was no study on Klotho improving cardiac remodeling after MI via AMPK/mTOR signaling. In this study, we found that Klotho had a protective effect on myocardial remodeling after myocardial infarction by regulating the AMPK/mTOR signaling pathway. However, this protective effect was then abolished after co-treatment with Compound C. It is possible that Klotho could improve cardiac function, fibrosis, inflammatory factors, ferroptosis, and oxidative stress in vivo and in vitro via the AMPK/mTOR signaling pathway.

Klotho's effect on cardiac remodeling in mice with MI could be explained by its regulation of AMPK/mTOR signaling. In contrast to our previous study [12], this study started Klotho treatment 1 week after MI, confirming that the mouse model had been successfully established. The treatment time we chose was more clinically appropriate. In addition, this study was the first to use an AMPK signaling pathway inhibitor to investigate the effects of Klotho on ferroptosis and oxidative stress. This study provided an alternative perspective regarding Klotho's mechanism of improving cardiac remodeling after MI.

Limitations

The present study has some limitations. On the one hand, the sample size was relatively small. On the other hand, the optimal dose of Klotho and Compound C has not been determined. Therefore, further studies are required to increase the sample size and to determine the optimal dose of Klotho and Compound C. Lastly, Compound C inhibits numerous other kinases other than AMPK with similar or greater potency. Further studies are needed to strengthen the conclusion that Klotho protects against cardiac dysfunction by regulating AMPK/mTOR signaling.

Conclusions

In conclusion, Klotho potentially improves cardiac remodeling in MI mice by regulating AMPK/mTOR signaling. These findings demonstrate Klotho as an effective MI therapeutic agent.

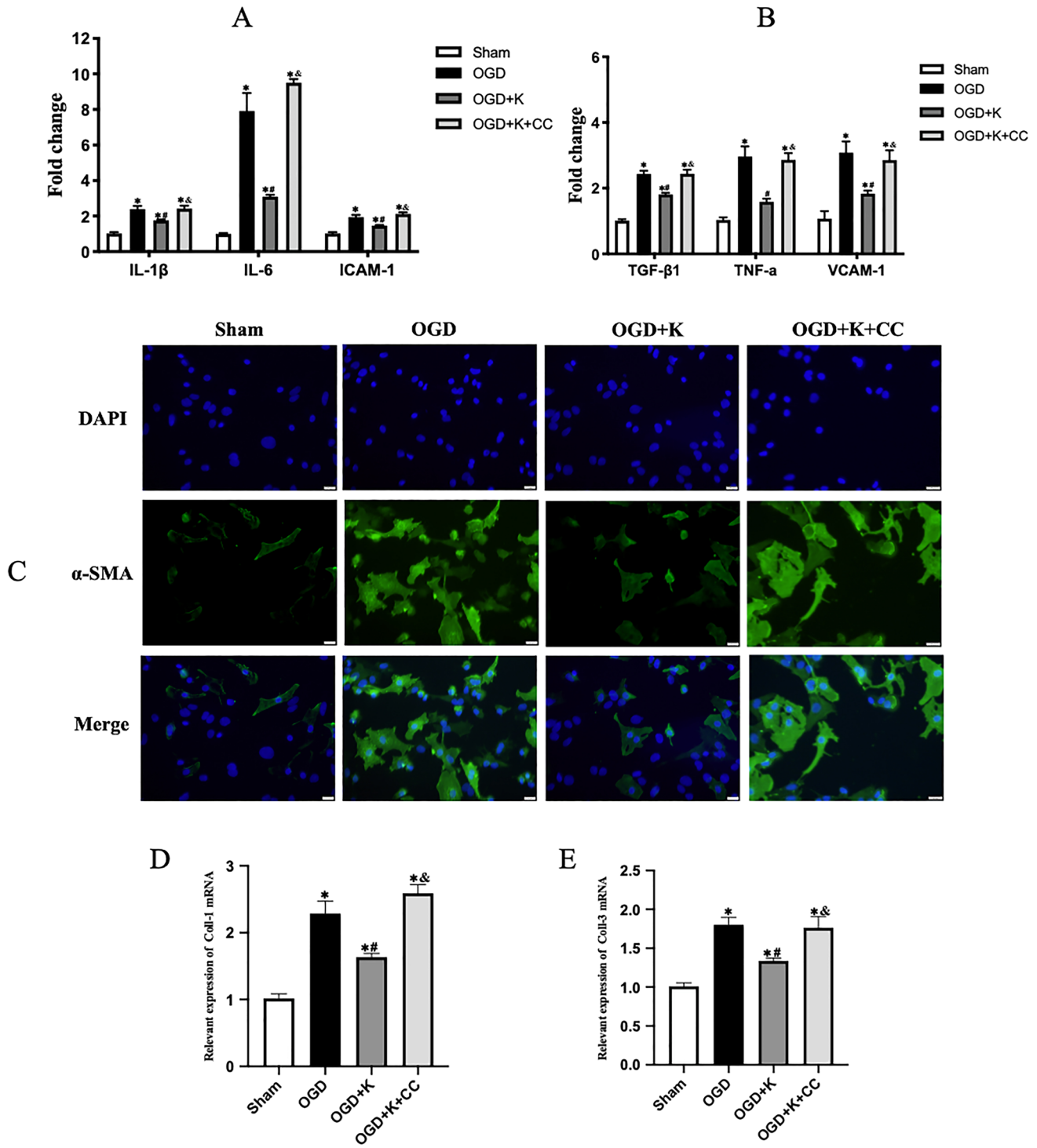

Fig. 5 Effects of Klotho on cardiac fibrosis and inflammatory cytokines in vitro. **A** Expressions of IL-1β, IL-6, and ICAM-1 mRNA. **B** Expressions of TGF-β1, TNF-α, and VCAM-1 mRNA. **C** Immunofluorescence staining of a-SMA in CFs. Scale bar: 20 μm. Expressions of Coll-1 (**D**) and Coll-3 (**E**) mRNA in CFs. Data are mean ± SEM. $^{*}P < 0.05$ vs. sham. $^{\#}P < 0.05$ vs. OGD. $^{\&}P < 0.05$ vs. OGD + K. CFs, cardiac fibroblasts; Coll-1, collagen I; Coll-3, collagen III; OGD, oxygen–glucose deprivation; K, Klotho; CC, Compound C

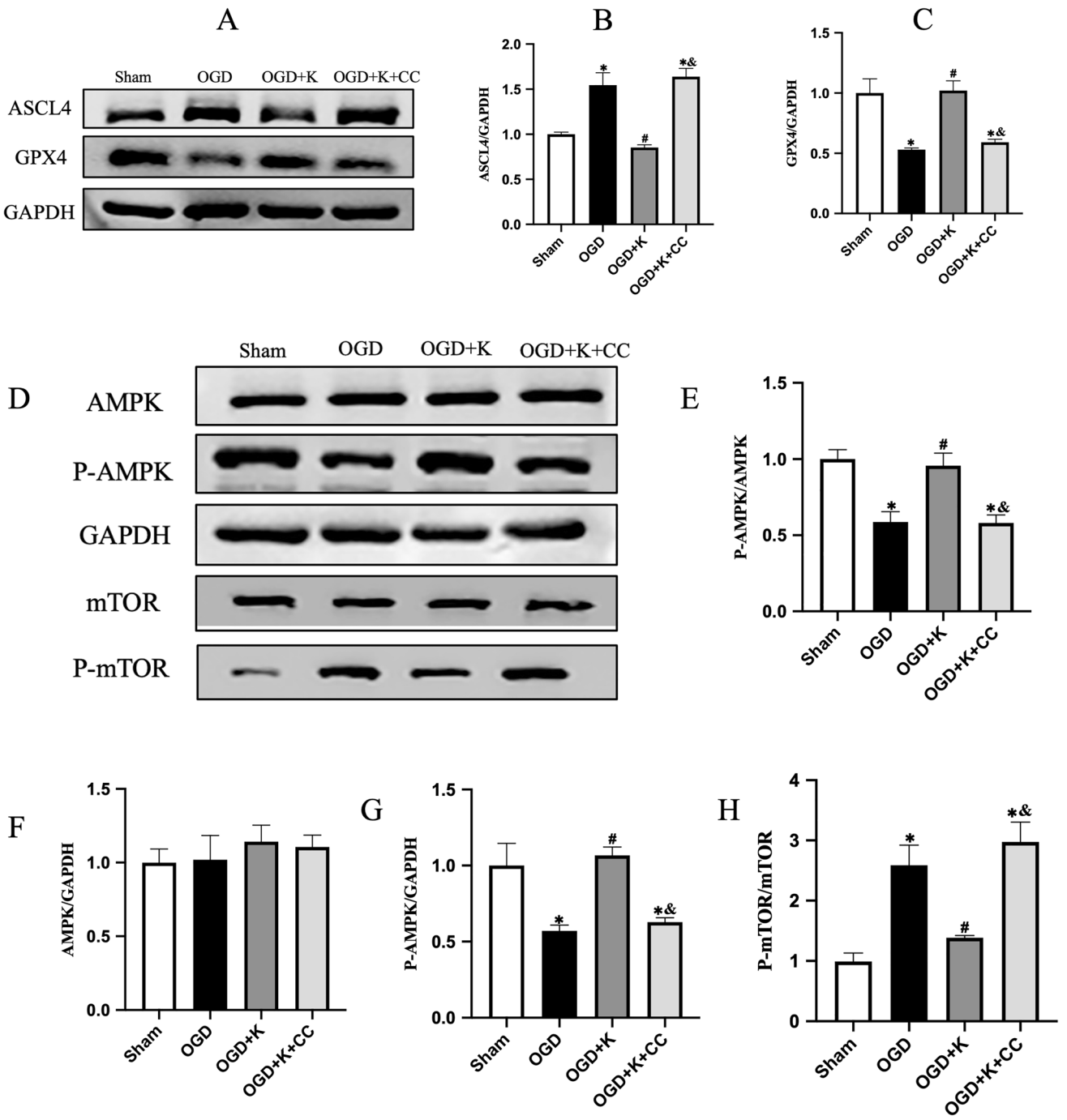

Fig. 6 Effects of Klotho on ferroptosis and AMPK/mTOR signaling in vitro. **A**–**C** Western blot analysis of the expressions of ASCL4 and GPX4. **D**–**H** Western blot analysis of the expressions of AMPK/mTOR signaling. Data are mean ± SEM. $^{*}P < 0.05$ vs. sham. $^{\#}P < 0.05$ vs. OGD. $^{\&}P < 0.05$ vs. OGD + K. OGD, oxygen–glucose deprivation; K, Klotho; CC, Compound C

Author contribution Kai WANG designed the study and completed the experiment together with Zhongming LI and Yinzhang DING. The first draft was written by Kai WANG, and the other authors participated in the revision and polishing of the draft. The authors declare that all data were generated in-house and that no paper mill was used.

Funding This work was supported by the National Natural Science Foundation of China (Grant No. 81871359 and No. 82071944).

Data Availability The data that support the findings of this study are available from the corresponding author upon reasonable request.

Declarations

Ethics approval The protocols for animal experiments followed NIH guidelines. Nanjing Medical University's ethics committee has approved the study (IACUC-2102002). ARRIVE guidelines were followed in the design of animal experiments.

Conflict of interest The authors declare no competing interests.

References

1. Wang K, Li Z, Sun Y et al (2021) Dapagliflozin improves cardiac function, remodeling, myocardial apoptosis, and inflammatory cytokines in mice with myocardial infarction. J Cardiovasc Transl Res, https://doi.org/10.1007/s12265-021-10192-y
2. Deng R, Liu Y, He H et al (2020) Haemin pre-treatment augments the cardiac protection of mesenchymal stem cells by inhibiting mitochondrial fission and improving survival. J Cell Mol Med 24:431–440. https://doi.org/10.1111/jcmm.14747
3. Talman V, Ruskoaho H (2016) Cardiac fibrosis in myocardial infarction-from repair and remodeling to regeneration. Cell Tissue Res 365:563–581. https://doi.org/10.1007/s00441-016-2431-9
4. Wang X, Guo Z, Ding Z et al (2018) Inflammation, autophagy, and apoptosis after myocardial infarction. J Am Heart Assoc 7: https://doi.org/10.1161/jaha.117.008024
5. Wu X, Li Y, Zhang S et al (2021) Ferroptosis as a novel therapeutic target for cardiovascular disease. Theranostics 11:3052–3059. https://doi.org/10.7150/thno.54113
6. Kurian GA, Rajagopal R, Vedantham S et al (2016) The role of oxidative stress in myocardial ischemia and reperfusion injury and remodeling: revisited. Oxid Med Cell Longev 2016:1656450. https://doi.org/10.1155/2016/1656450
7. Kuro-o M, Matsumura Y, Aizawa H et al (1997) Mutation of the mouse klotho gene leads to a syndrome resembling ageing. Nature 390:45–51. https://doi.org/10.1038/36285
8. Yamada S, Giachelli CM (2017) Vascular calcification in CKD-MBD: roles for phosphate, FGF23, and Klotho. Bone 100:87–93. https://doi.org/10.1016/j.bone.2016.11.012
9. Wang K, Mao Y, Lu M et al (2022) Association between serum klotho levels and the prevalence of diabetes among adults in the United States. Front Endocrinol (Lausanne) 13:1005553. https://doi.org/10.3389/fendo.2022.1005553
10. Chen K, Wang S, Sun QW et al (2021) Klotho deficiency causes heart aging via impairing the Nrf2-GR pathway. Circ Res 128:492–507. https://doi.org/10.1161/circresaha.120.317348
11. Guo Y, Zhuang X, Huang Z et al (2018) Klotho protects the heart from hyperglycemia-induced injury by inactivating ROS and NF-κB-mediated inflammation both in vitro and in vivo. Biochim Biophys Acta Mol Basis Dis 1864:238–251. https://doi.org/10.1016/j.bbadis.2017.09.029
12. Wang K, Zhongming LI, Yansong LI et al (2022) Cardioprotection of klotho against myocardial infarction-induced heart failure through inducing autophagy. Mech Ageing Dev. https://doi.org/10.1016/j.mad.2022.111714111714
13. Zhang X, Wang Q, Wang X et al (2019) Tanshinone IIA protects against heart failure post-myocardial infarction via AMPKs/mTOR-dependent autophagy pathway. Biomed Pharmacother 112:108599. https://doi.org/10.1016/j.biopha.2019.108599
14. Lu Q, Liu J, Li X et al (2020) Empagliflozin attenuates ischemia and reperfusion injury through LKB1/AMPK signaling pathway. Mol Cell Endocrinol 501:110642. https://doi.org/10.1016/j.mce.2019.110642
15. He Z, Zeng X, Zhou D et al (2021) lncRNA Chaer prevents cardiomyocyte apoptosis from acute myocardial infarction through AMPK activation. Front Pharmacol 12:649398. https://doi.org/10.3389/fphar.2021.649398
16. Yan J, Yan JY, Wang YX et al (2019) Spermidine-enhanced autophagic flux improves cardiac dysfunction following myocardial infarction by targeting the AMPK/mTOR signalling pathway. Br J Pharmacol 176:3126–3142. https://doi.org/10.1111/bph.14706
17. Ding J, Tang Q, Luo B et al (2019) Klotho inhibits angiotensin II-induced cardiac hypertrophy, fibrosis, and dysfunction in mice through suppression of transforming growth factor-β1 signaling pathway. Eur J Pharmacol 859:172549. https://doi.org/10.1016/j.ejphar.2019.172549
18. Wang F, Liu Y, Yuan J et al (2019) Compound C protects mice from HFD-induced obesity and nonalcoholic fatty liver disease. Int J Endocrinol 2019:3206587. https://doi.org/10.1155/2019/3206587
19. Benavides-Vallve C, Corbacho D, Iglesias-Garcia O et al (2012) New strategies for echocardiographic evaluation of left ventricular function in a mouse model of long-term myocardial infarction. PLoS One 7: e41691. https://doi.org/10.1371/journal.pone.0041691
20. Xu S, Mao Y, Wu J et al (2020) TGF-β/Smad and JAK/STAT pathways are involved in the anti-fibrotic effects of propylene glycol alginate sodium sulphate on hepatic fibrosis. J Cell Mol Med 24:5224–5237. https://doi.org/10.1111/jcmm.15175
21. Ge C, Zhao Y, Liang Y et al (2022) Silencing of TLR4 inhibits atrial fibrosis and susceptibility to atrial fibrillation via downregulation of NLRP3-TGF-β in spontaneously hypertensive rats. Dis Markers 2022:2466150. https://doi.org/10.1155/2022/2466150
22. Zhang Y, Liu S, Ding L et al (2021) Circ_0030235 knockdown protects H9c2 cells against OGD/R-induced injury via regulation of miR-526b. PeerJ 9:e11482. https://doi.org/10.7717/peerj.11482
23. Yang F, Qin Y, Wang Y et al (2019) Metformin inhibits the NLRP3 inflammasome via AMPK/mTOR-dependent effects in diabetic cardiomyopathy. Int J Biol Sci 15:1010–1019. https://doi.org/10.7150/ijbs.29680
24. Zhang M, Lei YS, Meng XW et al (2021) Iguratimod alleviates myocardial ischemia/reperfusion injury through inhibiting inflammatory response induced by cardiac fibroblast pyroptosis via COX2/NLRP3 signaling pathway. Front Cell Dev Biol 9:746317. https://doi.org/10.3389/fcell.2021.746317
25. Feng H, Mou SQ, Li WJ et al (2020) Resveratrol inhibits ischemia-induced myocardial senescence signals and NLRP3 inflammasome activation. Oxid Med Cell Longev 2020:2647807. https://doi.org/10.1155/2020/2647807
26. Xu C, Gao X, Wei Q et al (2018) Stem cell factor is selectively secreted by arterial endothelial cells in bone marrow. Nat Commun 9:2449. https://doi.org/10.1038/s41467-018-04726-3
27. Wang K, Li Z, Ma W et al (2021) Construction of miRNA-mRNA network reveals crucial miRNAs and genes in acute myocardial infarction. J Biomed Res 35:425–435. https://doi.org/10.7555/jbr.35.20210088
28. Zhang L, Cao M, Yu Z et al (2020) The restoration of Wnt/β-catenin signalling activity by a tuna backbone-derived peptide ameliorates hypoxia-induced cardiomyocyte injury. Am J Transl Res 12:5221–5236
29. Xu JP, Zeng RX, He MH et al (2022) Associations between serum soluble α-klotho and the prevalence of specific cardiovascular disease. Front Cardiovasc Med 9:899307. https://doi.org/10.3389/fcvm.2022.899307
30. Hongwei Y, Ruiping C, Yingyan F et al (2019) Effect of irbesartan on AGEs-RAGE and MMPs systems in rat type 2 diabetes myocardial-fibrosis model. Exp Biol Med (Maywood) 244:612–620. https://doi.org/10.1177/1535370219840981

31. Błyszczuk P, Zuppinger C, Costa A et al (2020) Activated cardiac fibroblasts control contraction of human fibrotic cardiac microtissues by a β-adrenoreceptor-dependent mechanism. Cells 9: https://doi.org/10.3390/cells9051270
32. Russo I, Frangogiannis NG (2016) Diabetes-associated cardiac fibrosis: cellular effectors, molecular mechanisms and therapeutic opportunities. J Mol Cell Cardiol 90:84–93. https://doi.org/10.1016/j.yjmcc.2015.12.011
33. Geelen T, Yeo SY, Paulis LE et al (2012) Internalization of paramagnetic phosphatidylserine-containing liposomes by macrophages. J Nanobiotechnol 10:37. https://doi.org/10.1186/1477-3155-10-37
34. Li A, Yu Y, Ding X et al (2020) miR-135b protects cardiomyocytes from infarction through restraining the NLRP3/caspase-1/IL-1β pathway. Int J Cardiol 307:137–145. https://doi.org/10.1016/j.ijcard.2019.09.055
35. Groot HE, Al Ali L, van der Horst ICC et al (2019) Plasma interleukin 6 levels are associated with cardiac function after ST-elevation myocardial infarction. Clin Res Cardiol 108:612–621. https://doi.org/10.1007/s00392-018-1387-z
36. Bradham WS, Moe G, Wendt KA et al (2002) TNF-alpha and myocardial matrix metalloproteinases in heart failure: relationship to LV remodeling. Am J Physiol Heart Circ Physiol 282:H1288-1295. https://doi.org/10.1152/ajpheart.00526.2001
37. Chen Q, Zhang D, Bi Y et al (2020) The protective effects of liguzinediol on congestive heart failure induced by myocardial infarction and its relative mechanism. Chin Med 15:63. https://doi.org/10.1186/s13020-020-00345-7
38. Chaar D, Dumont B, Vulesevic B et al (2021) Neutrophils pro-inflammatory and anti-inflammatory cytokine release in patients with heart failure and reduced ejection fraction. ESC Heart Fail 8:3855–3864. https://doi.org/10.1002/ehf2.13539
39. Li RL, Fan CH, Gong SY et al (2021) Effect and mechanism of LRP6 on cardiac myocyte ferroptosis in myocardial infarction. Oxid Med Cell Longev 2021:8963987. https://doi.org/10.1155/2021/8963987
40. Liu XJ, Lv YF, Cui WZ et al (2021) Icariin inhibits hypoxia/reoxygenation-induced ferroptosis of cardiomyocytes via regulation of the Nrf2/HO-1 signaling pathway. FEBS Open Bio 11:2966–2976. https://doi.org/10.1002/2211-5463.13276
41. Golej DL, Askari B, Kramer F et al (2011) Long-chain acyl-CoA synthetase 4 modulates prostaglandin E2 release from human arterial smooth muscle cells. J Lipid Res 52:782–793. https://doi.org/10.1194/jlr.M013292
42. Kagan VE, Mao G, Qu F et al (2017) Oxidized arachidonic and adrenic PEs navigate cells to ferroptosis. Nat Chem Biol 13:81–90. https://doi.org/10.1038/nchembio.2238
43. Xiang T, Luo X, Zeng C et al (2021) Klotho ameliorated cognitive deficits in a temporal lobe epilepsy rat model by inhibiting ferroptosis. Brain Res 1772:147668. https://doi.org/10.1016/j.brainres.2021.147668
44. Bugger H, Pfeil K (2020) Mitochondrial ROS in myocardial ischemia reperfusion and remodeling. Biochim Biophys Acta Mol Basis Dis 1866:165768. https://doi.org/10.1016/j.bbadis.2020.165768
45. Ma Z, Liu J, Li J et al (2020) Klotho ameliorates the onset and progression of cataract via suppressing oxidative stress and inflammation in the lens in streptozotocin-induced diabetic rats. Int Immunopharmacol 85:106582. https://doi.org/10.1016/j.intimp.2020.106582
46. Li MY, Zhu XL, Zhao BX et al (2019) Adrenomedullin alleviates the pyroptosis of Leydig cells by promoting autophagy via the ROS-AMPK-mTOR axis. Cell Death Dis 10:489. https://doi.org/10.1038/s41419-019-1728-5
47. Mihaylova MM, Shaw RJ (2011) The AMPK signalling pathway coordinates cell growth, autophagy and metabolism. Nat Cell Biol 13:1016–1023. https://doi.org/10.1038/ncb2329
48. Zhang J, Wang E, Zhang L et al (2021) PSPH induces cell autophagy and promotes cell proliferation and invasion in the hepatocellular carcinoma cell line Huh7 via the AMPK/mTOR/ULK1 signaling pathway. Cell Biol Int 45:305–319. https://doi.org/10.1002/cbin.11489
49. Ren PH, Zhang ZM, Wang P et al (2020) Yangxinkang tablet protects against cardiac dysfunction and remodelling after myocardial infarction in rats through inhibition of AMPK/mTOR-mediated autophagy. Pharm Biol 58:321–327. https://doi.org/10.1080/13880209.2020.1748662
50. Wang Z, Yao M, Jiang L et al (2022) Dexmedetomidine attenuates myocardial ischemia/reperfusion-induced ferroptosis via AMPK/GSK-3β/Nrf2 axis. Biomed Pharmacother 154:113572. https://doi.org/10.1016/j.biopha.2022.113572
51. Xue M, Yang F, Le Y et al (2021) Klotho protects against diabetic kidney disease via AMPK- and ERK-mediated autophagy. Acta Diabetol 58:1413–1423. https://doi.org/10.1007/s00592-021-01736-4